Author/s:
Keam, SP;Gulati, T;Gamell, C;Caramia, F;Huang, C;Schittenhelm, RB;Kleifeld, O;Neeson, PJ;Haupt, Y;Williams, SG

Title:
Exploring the oncoproteomic response of human prostate cancer to therapeutic radiation using data-independent acquisition (DIA) mass spectrometry

Date:
2018-06-01

Citation:
Keam, S. P., Gulati, T., Gamell, C., Caramia, F., Huang, C., Schittenhelm, R. B., Kleifeld, O., Neeson, P. J., Haupt, Y. & Williams, S. G. (2018). Exploring the oncoproteomic response of human prostate cancer to therapeutic radiation using data-independent acquisition (DIA) mass spectrometry. Prostate, 78 (8), pp.563-575. https://doi.org/10.1002/pros.23500.

Original Article

Exploring the oncoproteomic response of human prostate cancer to therapeutic radiation using data-independent acquisition (DIA) mass spectrometry[1].

Simon P. Keam 0000-0001-9053-9138 0000-0001-9053-9138[1*]

Simon.Keam@petermac.org

Twishi Gulati[1]	Twishi.Gulati@petermac.org
Cristina Gamell[1,2]	Cristina.Gamell@petermac.org
Franco Caramia[1]	Franco.Caramia@petermac.org
Cheng Huang[3]	cheng.huang@monash.edu
Ralf B. Schittenhelm[3]	ralf.schittenhelm@monash.edu
Oded Kleifeld[4]	okleifeld@technion.ac.il
Paul J. Neeson[2,6,7]	Paul.Neeson@petermac.org
Ygal Haupt[1,2,3,7#]	Ygal.Haupt@petermac.org
Scott G. Williams[5#]	Scott.Williams@petermac.org

[1]Tumor Suppression Laboratory, Peter MacCallum Cancer Centre, Melbourne, Victoria, Australia.

[2]The Sir Peter MacCallum Department of Oncology, The University of Melbourne, Melbourne, Victoria, Australia.

[3]Monash Biomedical Proteomics Facility, Biomedicine Discovery Institute and Department of Biochemistry and Molecular Biology, Monash University, Clayton, Victoria, Australia

[4]The Smoler Proteomics Center Technion – Israel Institute of Technology, Haifa, Israel.

[5]Division of Radiation Oncology and Cancer Imaging, Peter MacCallum Cancer Centre, Melbourne, Victoria, Australia.

[6]Cancer Immunology Research, Peter MacCallum Cancer Centre, Melbourne, Victoria, Australia.

[7]Department of Pathology, The University of Melbourne, Melbourne, Victoria, Australia.

*Corresponding author

Corresponding author contact details:

Email: Simon.Keam@petermac.org

Phone: +61 (038) 559-6471

[#]These authors contributed equally to this study

Running title

The oncoproteomic response of prostate cancer to radiation

Abbreviations used

PCa	prostate cancer
RT	radiation therapy
HDRBT	high-dose-rate brachytherapy
EBRT	external beam radiotherapy
ADT	androgen deprivation therapy
DIA	data-independent acquisition
MS	mass spectrometry

Declarations

Ethics approval and consent to participate

All participants provided consent covering tissue research as part of a prospective tissue collection study for prostate radiobiology research approved by the Human Research Ethics Committee at the Peter MacCallum Cancer Centre (PMCC; HREC approvals 10/68 and 13/167).

Consent for publication

Not applicable.

Availability of data and material

The datasets used and/or analysed during the current study are available from the corresponding author on reasonable request.

Competing interests

We have no conflicts of interest to disclose.

Funding

This study was funded by the PeterMac Foundation, the Victorian Cancer Agency, the Prostate Cancer Foundation USA (Creativity award), and by the Cancer Council Victoria (Grant-In-Aid).

Author contributions

S.K., S.W. and Y.H. conceived and designed the study. S.K. designed performed the experiments and analysed and the data. T.G., C.G., and C.H. assisted with experimental design. S.K and F.C. designed and performed the bioinformatics analyses. R.S. designed and

performed mass spectrometry and analysed the data. S.K. drafted the manuscript. S.K., R.S., O.K., P.N., C.G., S.W. and Y.H. critically revised the manuscript.

Acknowledgements

We would like to thank Professor Gail Risbridger from Peter MacCallum Cancer Centre, Professor Amanda Fosang from Murdoch Children's Research Institute, and Dr Michael Cater from Deakin University for their generous donation of antibodies for this study.

Abstract

Introduction

The development of radioresistance in prostate cancer (PCa) is an important clinical issue and is still largely uninformed by personalised molecular characteristics. The aim of this study was to establish a platform that describes the early oncoproteomic response of human prostate tissue to radiation therapy (RT) using a prospective human tissue cohort.

Methods

Fresh and fixed transperineal biopsies from eight men with clinically localised tumours were taken prior to and 14 days following a single fraction of high-dose-rate brachytherapy. Quantitative protein analysis was achieved using an optimised protein extraction pipeline and subsequent data-independent acquisition mass spectroscopy (DIA-MS). Ontology analyses were used to identify enriched functional pathways, with the candidates further interrogated in formalin-fixed paraffin-embedded tissue biopsies from five additional patients.

Results

We obtained a mean coverage of 5,660 proteins from fresh tissue biopsies; with the principal post-radiation change observed being an increase in levels amongst a total of 49 proteins exhibiting abundance changes. Many of these changes in abundance varied between patients and, typically to prostate cancer tissue, exhibited a high level of heterogeneity. Ontological analysis revealed the enrichment of the protein activation cascades of three immunological pathways: humoral immune response, leukocyte mediated immunity and complement activation. These were predominantly associated with the extracellular space. We validated significant expression differences in between 20% and 61% of these candidates using the separate fixed-tissue cohort and established their feasibility as an experimental tissue resource by acquiring quantitative data for a mean of 5,152 proteins per patient.

Discussion

In this prospective study, we have established a sensitive and reliable oncoproteomic pipeline for the analysis of both fresh and formalin-fixed human PCa tissue. We identified multiple pathways known to be radiation-responsive and have established a powerful database of candidates and pathways with no current association with RT. This information may be beneficial in the advancement of personalised therapies and potentially, predictive biomarkers.

Introduction

Approximately one in seven men will be diagnosed with prostate cancer (PCa) in their lifetimes which is then responsible for more than 300,000 deaths globally annually. The prevalence of early detection methods means that most cases can be treated early and successfully with standardised radical therapies, including radiation therapy (RT) and prostatectomy[1]. Despite high cancer control rates, radio-resistance still occurs in many cases treated with RT[2]. Our understanding of the processes that drive cell death in response to radiation have, however, predominately focussed on *in vitro* or animal models of PCa. The absence of data analysing the response of the human prostate to radiation therapy has largely been driven by the difficulty associated with obtaining prospective comparative tissue samples to enable differential profiling.

The field of high-throughput radio-proteomics has emerged as a powerful tool to define protein changes in response to RT with the extraction of clinically useful biomarkers in mind[3]. However, the absence of surrounding tissue- and human immune-context information in these studies has meant application to a clinical setting has been difficult. We hypothesised that radiation-induced proteomic changes within tumours may yield valuable insight into the causes of different treatment outcomes observed clinically. In this study, we aimed to characterise the proteomic response of human PCa to radiation *in situ*. This is made

possible by a prospective tissue acquisition study specifically designed to address radiobiology questions in PCa. Matched PCa biopsies prior to and following RT were obtained and processed specifically for quantitative proteomic analysis. We report the first pilot proteomic data from this novel cohort, assess the major pathways perturbed following RT, and validate expression changes in fixed archival tissue. We conclude that this is a powerful means of revealing novel insights into the response of human PCa tissue to RT, paving the way for clinically-relevant target selection and means for the mitigation of radioresistance for improved therapeutic outcomes.

Methods

Cohort characteristics

Table 1 shows the clinical characteristics of the eight patients with intermediate risk, localised PCa analysed. Each received high-dose-rate brachytherapy (HDRBT) with curative intent as a boost therapy prior to external beam radiotherapy (EBRT) using an afterloaded Iridium-192 (^{192}Ir) source (Elekta Flexitron). Brachytherapy was performed using transrectal ultrasound guidance and computed tomography simulation for planning purposes. Patients had two HDRBT treatments performed 14 days apart with a 10Gy fraction prescribed to the target volume (whole prostate) on each occasion, followed by 46Gy in 23 fractions of EBRT. Androgen Deprivation Therapy (ADT) was not employed in any of these cases. All participants provided consent covering tissue research as part of a prospective tissue collection study for prostate radiobiology research approved by the Human Research Ethics Committee at the Peter MacCallum Cancer Centre (PMCC; HREC approvals 10/68 and 13/167).

Tissue collection and processing

Transperineal ultrasound-guided prostate biopsies were obtained using a 16G biopsy system (Bard Magnum series) both immediately before the first fraction of HDRBT and again 14

days later. Each paired sample set therefore represents the 14 day response to a single 10Gy fraction of HDRBT. Each tissue collection was comprised of three to five biopsies directed at a region known to be tumour-bearing based on prior MRI or PET scanning or biopsy data (where available) the location of a nodule on examination; and any region of abnormality on ultrasound at the time of biopsy. Integration of all of these clinical and imaging factors was performed at the time of biopsy ("cognitive fusion") by the procedural clinician. Tissue cores were either snap frozen at -80°C or fixed immediately by immersion in a solution of 10% neutral buffered formaldehyde for a maximum of 24 h at room temperature prior to paraffin-embedding. Representative 3µm sections were acquired from all paraffin blocks for routine staining for light microscopy and high-resolution scanning. For both pre- and post-radiation tissues, representative hemotoxylin and eosin stains, and PIN4 triple-stains, are included in Supplementary Figures S1 and S2, respectively. Cases were specifically chosen for this study based on assessment of tumour burden within biopsied tissue (≥50% cutoff) and an absence of necrotic features.

Tissue lysis and protein extraction and preparation for mass spectrometry

Fresh tissue cores were snap-frozen and stored at -80°C immediately after extraction from patients. For protein extraction, each core was diced whilst frozen using a clean scalpel, to which 100 µl of 1% w/v sodium deoxycholate (Sigma, D6750-100G) buffer (1% w/v SDC, 100 mM Tris pH 8.1) was added and the tissue was homogenised using five cycles at amplitude 10 on a Soniprep 150 Plus sonicator (MSE). Protein concentration was assessed via bicinchoninic acid assay (Pierce, Cat#23225) prior to protease digestion. For DIA-MS analysis, 300 µg of total protein was denatured by adding TCEP (Thermo, Cat#:77720) to a concentration of 10 mM for 30 min at 50°C. Free cysteine residues were alkylated for 20 min at RT in the dark using 40 mM chloroacetamide (Sigma, C0267-100G) and the proteins were digested with MS-grade trypsin (Promega, Cat#:V5280) at 37°C overnight with mild shaking.

Digestion was stopped by the addition of formic acid to a final concentration of 1% v/v. SDC removal was achieved by adding an equal volume of water-saturated ethyl-acetate followed by thorough vortexing. The solution was centrifuged at full speed and the middle aqueous layer removed to a fresh tube. This step was repeated twice.

For analysis of formalin fixed tissue, protein lysate was obtained from single 10 µm tissue sections using a Qproteome FFPE tissue kit (Qiagen, Cat#:37623) and processed according to the manufacturer's instructions for mass spectrometric analyses.

For analysis of both fresh and fixed specimens, the digested peptide solution was then vacuum centrifuged at 30°C to pellet peptides which was then resuspend in 30 µl buffer A (0.1% formic acid in ddH_2O). Purification and desalting of peptides was performed using P-10 ZipTip columns (Agilent, OMIX-Mini Bed 96 C18, A57003MBK) which were eluted in 30 µl Buffer B (50% acetonitrile, 0.1% formic acid in ddH_2O) according to the manufacturer's instructions. Eluted peptides were then vacuumed centrifuge dry and resuspended in 20 µl buffer A containing the iRT peptides[4].

Experimental Design and Statistical Rationale

Radiation-specific changes were identified by amalgamating and comparing 3-5 replicate biopsies at pre-clinical or post-radiation timepoints in each of eight patients (n = 8). This approach limited biopsy-specific effects due to inherent and unavoidable tissue heterogeneity. Matched pair analysis was used to identify proteins with altered levels post-radiation. Fresh tissue from three patients (n = 3) was used to generate a list of preliminary changes which was subsequently validated in fixed tissue sets (n = 7). Full details of protein recovery and protein number identification can be found in Supplementary Table S1. This approach was designed to limit any potential bias resulting from the fixation process and give the best chance of identifying biologically relevant candidates in unfixed fresh tissue. Study design and sample size permitted a false positive rate =1%, power of 0.9, $|\mu_1|= 0.584$ and $\sigma_d = 0.3$.

Combined statistical analyses were performed using Spectronaut Orion (Biognosys) merged pre-clinical and post-radiation samples used thresholds $\log_2$ fold change of 0.584 and *q* value < 0.05 following analysis of multiple patient pairs and normalization using median abundances of all peptides/proteins.

Data-dependent acquisition (DDA) mass spectrometry

Using a Dionex UltiMate 3000 RSLCnano system equipped with a Dionex UltiMate 3000 RS autosampler, the samples were loaded via an Acclaim PepMap 100 trap column (100 µm x 2 cm, nanoViper, C18, 5 µm, 100Å; Thermo Scientific) onto an Acclaim PepMap RSLC analytical column (75 µm x 50 cm, nanoViper, C18, 2 µm, 100Å; Thermo Scientific). The peptides were separated by increasing concentrations of 80% ACN / 0.1% FA at a flow of 250 nl/min for 158 min and analyzed with an Orbitrap Fusion Tribrid mass spectrometer (Thermo Scientific). Each cycle was set to a fixed cycle time of 4 sec consisting of an Orbitrap full ms1 scan (resolution: 120.000; AGC target: 1e6; maximum IT: 54 ms; scan range: 375-1575 m/z) followed by several Orbitrap ms2 scans (resolution: 30.000; AGC target: 4e5; maximum IT: 118 ms; isolation window: 1.4 m/z; HCD Collision Energy: 32%). To minimize repeated sequencing of the same peptides, the dynamic exclusion was set to 15 sec and the 'exclude isotopes' option was activated.

Quantification of proteins using data-independent acquisition (DIA) mass spectrometry

The identical instrument setup as described above (Dionex UltiMate 3000 LC system coupled to an Orbitrap Fusion Tribrid mass spectrometer) has been used to quantify proteins using data-independent acquisition (DIA). 50 sequential DIA windows with an isolation width of 12 m/z between 375 - 975 m/z have been acquired in 2 consecutive injections (resolution: 30.000; AGC target: 1e6; maximum IT: 54 ms; HCD Collision energy: 32%; scan range: 200-2000 m/z) following a full ms1 scan (resolution: 120.000; AGC target: 1e6; maximum

IT: 54 ms; scan range: 375-1575 m/z). A 158 min gradient of increasing concentrations of 80% ACN / 0.1% FA has been used to separate the peptides for the DIA acquisition.

Mass spectrometric data analysis

Acquired DDA .raw files were searched against the human UniProtKB/SwissProt database (v2016_07) containing 20,221 entries including the iRT peptide sequences [4] using Byonic (Protein Metrics) embedded into Proteome Discoverer (Thermo Scientific) to obtain peptide sequence information. The following search parameters and settings have been used: (i) decoys and contaminants were added through Byonic, (ii) trypsin (full specificity after R and K) was selected as protease and up to 2 missed cleavages were permitted; (ii) mass tolerances were set to 10 and 20 ppm for precursor and fragment masses, respectively; (iii) Carbamidomethylation of cysteine residues was selected as fixed modification; (iv) oxidation of methionine residues was the only variable modification permitted; (v) both wildcard searches and glycan modifications were disabled. Only peptides identified at a false discovery rate (FDR) of 1% based on the added decoy database were considered for further analysis.

Spectronaut 10 (Orion; Biognosys) was used to create the corresponding spectral library based on the Proteome Discoverer output files. All DIA raw files were converted to the HTRMS file format using the HTRMS converter (Biognosys) and evaluated with Spectronaut 10 using default, protein-centric parameters (BGS Factory Settings). Data matrices containing the quantitative values were obtained for both “QValue” and “QValue Sparse” data filters, which are implemented in Spectronaut. Raw Spectronaut .sne files have been deposited as supplemental data and can be inspected with Biognosys Spectronaut Viewer.

Bioinformatic analyses

Hierarchical clustering (HC) and principal component analyses (PCA) were performed using the Perseus computational platform[5]. HC data were generated using Euclidean distance,

average linkage and k-means pre-processing by default on normalized protein values for relevant proteins or subsets of proteins. To identify proteins with either increased or decreased relative abundance following radiation relative to pre-radiation state, a fold difference between post- over pre-radiation protein values was used to identify relative transcript abundance. High-confidence lists were generated comprising proteins that exhibited $\log_2$ fold-changes in post-radiation sample ≥ 0.584 (upregulated) or ≤ 0.584 (downregulated) normalised protein quantification values relative to pre-radiation. High-confidence proteins lists were generated by identification of common changes with shared directionality in all three patients. Protein list enrichment analysis was performed using a variety of software platforms. Kyoto Encyclopaedia of Gene and Genomes (KEGG) enrichment was performed using the KEGG pathway database[6-8] and analysed using online Enrichr software[9, 10]. An adjusted *p* value threshold of 0.05 was used for pathway discovery. Results are presented as significance ($-\log_{10}$ transformed) and percentage of pathway proteins identified in relevant protein set. Molecular function, biological process and cell compartment enrichment analysis was performed using the Gene Ontology Consortium database[11, 12] and analyzed using Panther [13]. A *p* value threshold of 0.05 used for enrichment discovery with Benjamin-Hochberg method correction for multiple testing and used custom background dataset comprising 8,007 proteins covered by a custom spectral library database . Results were presented as significance ($-\log_{10}$ transformed) and percentage of pathway proteins identified in relevant protein set. Functional network analysis was performed using Cytoscape software [14] with ClueGO plug-in[15] on groups of proteins with increased or decreased abundance with clustering on basis of shared ontology groups. Ontology *pV* value threshold used was 0.001 and kappa = 0.51.

Western blot and antibodies

Immunoblotting was performed as previously described [16]. 2 µg of total protein was analysed with commercial antibodies to Ferritin (Abcam, ab-75973), Prostatic Acid Phosphatase (Abcam; ab-109004) and Fibrinogen γ (Santa Cruz, sc-133226).

Results

Experimental design, protein quantification and cluster analyses

This study was conducted in two phases as outlined in Figure 1A: (Phase I) a discovery phase to identify proteomic changes and radiation-responsive proteins in fresh tissue, and (Phase II) a validation phase to confirm the phase I findings in fixed tissues. In order to describe the proteomic response of prostate cancer cells to ionising radiation, we generated a dataset of highly conserved proteomic changes using fresh prostate cancer biopsies harvested from three patients immediately prior to and 14 days after a single 10 Gy dose of image-guided HDRB. For the initial discovery phase (Phase I), we used fresh-frozen tissue biopsies from three patients (RB031, RB038, RB045) taken immediately before and 14 days post-radiation and quantified protein abundances using data-independent acquisition mass spectrometry (DIA-MS). An in-house generated spectral library from human prostate tissue was used to interrogate all DIA raw files (data not shown). Following normalisation and imputation, we obtained quantitative data for 6,235, 5,110 and 5,628 proteins using fresh tissue from patients RB031, RB038 and RB045, respectively. To determine if the effects of radiation exposure can be predicted from the overall proteomic change, we performed hierarchical and 2-component PCA analysis on the normalized expression data from all six datasets. The results, shown in Figure 1B and C, revealed that radiation-specific clustering was largely absent and instead indicated patient-specific heterogeneity. The two components within PCA analysis accounted for 91.1% of the variation observed.

Identification of RT-sensitive candidate proteins

To identify proteins with either induced or repressed expression in response to radiation, we generated $\log_2$ differences of individual protein abundance post-radiation compared to pre-radiation and filtered the data for proteins that exceeded differences of +0.58 (increased expression) or -0.58 (decreased expression) which are equivalent to fold-change cut-offs of 1.5. Using this approach, we identified a total of 1086, 376 and 184 proteins with significantly altered expression in patients RB031, RB038 and RB045, respectively (Figure 2A). A parallel statistical analysis of grouped pre-treated and post-radiation samples identified 264 candidates (Figure S4A, $p < 0.05$; 1.5-fold change). However, this analysis was not used for candidate identification as it is geared toward universal radiation responses rather than those that are patient-specific and/or highly variable, which are the most clinically useful.

Despite the indicated patient-specific variation within the datasets, 49 radiation-responsive proteins were independently identified in all three patients regardless of directionality. Stratification of these candidates as either increasing or decreased in abundance (shown in Figure 2B and C), revealed that 27 of the 49 (55%) were of a uniform direction in all patients - being biased toward those increasing (24 proteins) rather than decreasing (3 proteins) in abundance. Those increasing with the highest average change included Ferritin Light Chain, Tenascin C, Keratin 15, CD163 and the Alpha, Beta and Gamma chains of Fibrinogen. Proteins with the most decreased levels included Ras GTPase-Activating-like Protein IQGAP2, Prostatic Acid Phosphatase and ATP-Citrate Lyase. 22 candidates, including Lactotransferrin and Myeloperoxidase, exhibited divergent patient-specific fold changes. The accurate identification of candidates was supported by immunoblot analysis of abundance changes for Fibrinogen γ, Ferritin, and Prostatic acid phosphatase in pre- and post-radiation total protein lysates from RB031, RB038 and RB045 (Supplementary Figure S3). Importantly, these recapitulated both the directionality and relative magnitude of changes

observed. A list of these patient-specific fold changes and functional classification of the 27 high-confidence candidates with similar directionality in all three patients is provided in Table 2. Broad classification of the candidates revealed that secreted glycoproteins, iron storage macromolecules and type I cytokeratins were amongst the proteins with the highest average fold changes (>4-fold difference).

Ontologically enriched pathways following radiation

The second phase of our study had the primary aims of identifying what cellular pathways are perturbed by radiation and determine if they are conserved in an extended cohort of fixed tissue specimens. To do this, we performed gene ontology analyses using a dataset of candidates that exhibited significant variation in at least 2 of the 3 patients (312 proteins). This was done to include proteins which may exhibit inconsistent expression and thus potentially include useful markers of variable radiation responses, including radioresistance. Using the gene ontology consortium database of biological processes, molecular functions and cell compartment ontologies, we identified 196, 44 and 63 significant ($p < 0.05$) hits in each category, respectively (see Supplementary Tables S2-4 for full lists). Biological processes that were most overrepresented in the data included the protein activation cascade, defence response, humoral immune response, leukocyte mediated immunity and complement activation (Figure 3A). Numerous molecular functions were also highly enriched amongst the candidates, specifically those involving proteolytic enzymes and their regulatory pathways, including peptidase regulator activity, serine-type endopeptidase activity, serine-type peptidase activity, serine hydrolase activity and endopeptidase inhibitor activity (Figure 3B). Analysis of the underlying protein types contributing to these enrichments revealed a collection of 22 proteins comprising Serpins (e.g. SERPH3), inter-α trypsin inhibitors (e.g. ITIH3), complement proteins (e.g. CO3), metalloproteases (e.g. TIMP3), collagen (e.g. CO7A1) and apolipoproteins (e.g. APOA2), amongst others.

Finally, when determining which cell compartments were enriched, we identified that the interstitium was overrepresented – most significantly for ontologies for extracellular space, blood microparticle, extracellular region part, extracellular exosome and extracellular organelle (Figure 3C). An additional analysis using the curated KEGG database reveals a highly significantly enrichment for the Complement and coagulation cascade pathway (Supplementary Figure S5 and Table S5). Finally, we performed a ClueGO analysis using to decipher functional connections between overrepresented ontologies and determine those with the most enriched terms. The results, shown in Figure 3D, indicated that wounding healing, inflammation and endopeptidase activity all share a similar underlying functionally connected network. Surprisingly, all other terms were relatively unconnected, including immune activation, apoptotic cell clearance, blood vessel development and catabolism. These data highlight the variety and scope of pathways likely to be the most responsive to radiation.

Validation of preliminary candidates in formalin-fixed tissue cohort

The current candidates were generated using fresh frozen tissue from a cohort of three patients. However, the bulk of tissue in the RadBank cohort is comprised of prospective formalin-fixed paraffin-embedded material. It was therefore imperative to demonstrate that changes identified at the fresh tissue level are maintained in fixed tissues. To do this, we isolated total protein from single 10µm sections of 15G (1.37 mm inner diameter) FFPE tissue core biopsies from two patients already analysed using fresh tissue (RB031 and RB038), plus five additional patients with similar characteristics (RB06, RB08, RB16, RB19 and RB20). These were processed and analysed in a similar fashion to fresh tissue analysis. Despite likely degradation and irreversible modifications as a result of the fixation process, we achieved excellent and consistent proteomic coverage of 5,152 ± 178 proteins amongst the 7 pairs of pre-treatment and post-radiation tissues. In order to determine the robustness of our protein purification and DIA quantification method, we compared both the total protein

coverage and candidates identified using FFPE tissue with matching (RB031 and RB038) fresh tissue counterparts. The results, shown in Supplementary Figure S6, demonstrated that between 87.7% and 95.7% of FFPE proteins were also quantified in fresh tissue libraries, and similarly that between 49.6% and 57.5% of the individual candidates were also shared. This result highlights the capacity of our analysis pipeline to reliably assess protein abundance in FFPE tissues.

These data were then used to confirm the changes in the 49 candidates generated in the first phase of the study. The results, outlined in Table 3 and illustrated in Figure 4A and B, demonstrated that between 20.4 and 65.3% of the candidates were confirmed in each of the new FFPE patient pairs. We verified that the total quantified proteomic library size does not influence the number of candidates validated, as shown in Supplementary Figure S7A (R^2 = 0.000020). However, we did identify a correlation (R^2 = 0.55) between validation success and number of candidates from each patient (Supplementary Figure S7B). In a parallel analysis, we grouped pre- and post-radiation FFPE tissues (analysed contemporaneously) in order to identify statistically significant candidates that may not necessarily exhibit large fold-changes in all patients (Figure S1B). Using this merged analysis, we identified a total of 464 statistically significant candidates which included 25/49 (51%) and 132/264 (50%) of the candidates obtained by either patient-specific or combined replicate analysis in Phase I, respectively (Figure 4 and Figure S1C).

This result highlighted that many candidates exhibit lower fold-changes in fixed tissue and thus escaped validation using stringent fold-change thresholds. Analysing the enrichments in biological process, molecular function and cell compartment ontologies from FFPE candidates alone revealed that 67%, 63% and 90% were shared with those found in fresh tissue analysis (Supplementary Figure S8).

The 49 candidates identified previously were then grouped into five classes based both the proportion validated in each of the seven FFPE patient pair analyses and statistical validation from grouped analyses: (i) highest confidence (all 7 pairs identified and S.V; statistical validation) (ii) high confidence (S.V only), (iii) moderate confidence (6 patients only), (iv) low confidence (1-5 patients) and (v) no confidence (no patients). Using these criteria, we identified six candidates at the highest confidence, including Tenascin C, Fibrinogen Alpha, Fibrinogen Beta, Fibrinogen Gamma, Fibronectin 1 and Complement Factor B. Statistical analysis revealed 19 additional proteins in the high statistical confidence category but did not necessarily meet the strict fold change requirements for the top category. Additional validated proteins with increased abundance in this category included Ferritin Light Chain, Keratin 15, CD163, Ferredoxin Reductase, Cathepsin B and HLA class II histocompatibility antigen (DRα chain). Statistical analysis also validated four proteins with decreased levels that were not observed in the highest confidence category. These included Protein and Arginine-Rich End Leucine Rich Repeat Protein, RAB27B, Prostatic Acid Phosphotase and Ras GTPase-Activating-like Protein IQGAP2. One additional protein, Lactotransferrin, was in the moderate confidence category but exhibited divergent expression differences that were dependent on the patient analysed – congruent what was observed in fresh tissue. Only on one occasion could a candidate, Complement C7, not be quantified in an FFPE patient pair (RB031) and two proteins, Stratifin and Sarcoglycan Delta, were not validated in any of the fixed tissues.

Sample type-specific variation was of interest for our investigation as we were interested in the effect of fixation on protein identification. Therefore, we compared matching fresh and fixed samples collected concurrently from two patients (RB031 and RB038) and established that 61.2% and 55.2% of the protein changes could be identified again. Importantly, only two

of these proteins exhibited disparate directionality to the fresh tissue analysis (RB038; S100 Calcium binding protein A9 and Plastin 3).

Finally, we were interested in response of known PCa markers that are currently used in the diagnosis and tracking of disease, shown in Supplementary Figure S9. The results indicated that PSA and FAS were almost universally downregulated to some degree in all patient samples following radiation. However, AR, PSMA, hK2 and IGF1 were either less consistent or could not be identified, suggesting that changes in their abundance are patient-specific and less likely to be strongly linked to radiation exposure.

Discussion

Due to the difficulty in accessing matched pre- and post-radiation human tumour tissue, the bulk of research into radiation-induced proteomic changes and mechanisms of resistance of human tumours has predominately focused on those that are detectible in human sera, urine, animal models and *in vitro* model systems (for review see[3]). Unfortunately, these types of analyses cannot determine differences in local tissue effects of radiation exposure, nor take into account the contribution of the tumour microenvironment. To the best of our knowledge, our study represents the first analysis of proteomic changes resulting from clinical radiation monotherapy *in situ*. Our unique prospective tissue cohort permitted the discovery and validation of numerous candidate proteins and pathways whose abundance is consistently perturbed following radiation.

Using fresh biopsy tissue collected immediately before and two weeks following radiation, we performed data-independent mass spectroscopy and observed proteomic profiles that were far more indicative of patient source than radiation state. Despite this, we identified a core group of 49 proteins which exhibited differential protein abundances in all patients. We also observed a predisposition for an increase, rather than a decrease, in the abundance of these proteins following radiation - potentially indicative of proteins expressed in infiltrative

immune cells or as part of scaffold repair. In addition to validating expression changes in approximately half of the fresh tissue candidates, our DIA-MS pipeline also consistently quantified >5,000 proteins from a relatively small amount of tissue. This was comparable with our fresh tissue resource and improves upon previous analyses of fixed prostatic tissue [17].

These FFPE analyses also produced a separate candidate list which enriched for the vast majority of ontologies also observed in fresh tissue candidates. This suggests that whilst individual protein abundance changes may not necessary be highly conserved, there is a high degree of similarity between pathways that are overrepresented between sample types.

Nevertheless, a small group of five glycoproteins, including tenascin C, fibronectin and the complete fibrinogen hexamer (consisting of subunits α, β and γ) complex, also known as factor I, were consistently more abundant and had the greatest magnitude of change. We posit that the increased abundance of these types of proteins is likely due to a combination of wound-healing responses and increased production of supportive tissue during a regenerative remodelling phase[18-20]. These observations were congruent with enriched ontologies amongst the conserved protein changes. Many of the ontologies that were enriched have well-described roles in processes known to be perturbed by ionising radiation, including cellular defence[21, 22], innate immune activation[22] and initiation of the complement cascade[23].

Previously reported studies of circulating serum markers of radiation in PCa in two different laboratories have demonstrated the upregulation of pro-inflammatory and coagulation-related proteins that were represented by similar paralogs in this study. Specifically, Complement protein 6 and Apolipoprotein A2[24], or Apolipoprotein A1[25] were upregulated following either intensity-modulated RT or EBRT, respectively. The common identification of these types of proteins in both the sera and tumour tissue of irradiated patients sheds light on the

systemic effects of localised radiation and escape of cells/molecules from the tumour bed following RT.

Other proteins with significant differential abundances have been previously determined to be radiation-responsive (in some cases radio-protective), including Ras GTPase-activating-like protein IQGAP2[26], Lactotransferrin[27], Serpin Family H Member 1/Hsp47[28] and Ferrodoxin Reductase[29]. Statistical identification of radiation-response proteins also recapitulated several putative protein drivers of radiation resistance recently discovered in *in vitro* models of prostate cancer [30]. These included Methylcrotonoyl-CoA carboxylase subunit alpha (*MCCC1*), 60 kDa heat shock protein (*HSPD1*), Alpha-2-HS-glycoprotein (*AHSG*) and Histidine Triad Nucleotide Binding Protein 1 (*HINT1*). These were not identified as bona-fide candidates in our analysis due to the thresholds imposed. The absence of many of these novel drivers is likely to be a product of increased variability resulting from the analysis of heterogeneous tissue sources.

Using a global view, we observed the enrichment of ontologies for humoral immune activation, complement activation, leukocyte-mediated immunity and blood vessel development. Several pro-inflammatory and immune-related proteins with increased abundance were also identified, including CD163, Cathepsins, Myeloperoxidase, S100 Calcium Binding Proteins (Calprotectins) and HLA class II histocompatibility antigen DRα chain. These are strong indicators of macrophage and myeloid cell activation and function, potentially resulting from RT-induced myeloid cell infiltration [31]. Additionally, there was an overrepresentation of proteins strongly linked to serine protease activity - a well-described functional element of the innate immune system in driving blood coagulation, inflammation, apoptosis and tissue remodelling[32]. The indication of increased proteolytic activity is also highly relevant to the progression of numerous malignancies, including that of prostate cancer [33, 34]. These results are also consistent with the observation that the candidates are

most highly expressed in the extracellular space; matching the majority of the putative ontological functions. Overall, this is consistent with the known features of new tissue deposition and remodelling as relatively late effects of RT on tumour and supportive tissue[35].

The primary aims of this pilot study were to recapitulate the known radiation response context and define the most perturbed pathways using an unbiased proteomic approach. We utilised recently established technologies that enable fresh tissue comparisons for proteomic discovery and follow-up validation in fixed tissues[36]. A limitation of this study was highlighted by the inability to validate many of the expression changes of numerous candidates in fixed tissues; even those sourced from the same patient simultaneously at the time of biopsy. This is likely a result of a combination of known issues regarding the heterogeneity of PCa tissue, limitations on repeated biopsy accuracy and complications inherent to the fixation procedure that can result in >20% of proteins being inaccessible to detection[36]. At present, limited emphasis should be placed on the individual proteins identified and instead constrained to pathways overrepresented. An additional caveat is that our study was not designed to identify proteins that exhibit highly variable expression patterns and are potentially the most useful as biomarkers. This highlights the need for further research with additional patients that will increase the statistical confidence in candidates and power to identify biomarkers. The need for additional prognostic and predictive markers of PCa RT responses is also highlighted here by the inconsistency of selected previously reported PCa biomarkers such as PSMA and androgen receptor expression. Although PSA and FAS demonstrated the potential for utility, these will require further work to establish if they are adaptable to the context of radiation therapy.

A final unexplored question for radiobiology research in PCa is the contribution of normal adjacent tissue, tumour-cell responses and infiltrating cell/serum responses to the overall

tissue response. Our pilot data represents a valuable resource for the identification of core mechanisms integral to the radiation response of both PCa and surrounding tissue, but may also have value in future studies aimed at differentiating the spectra of therapeutic responses observed clinically. However, our study is currently limited by the lack of therapeutic response and patient outcome data, which is still several years from maturation, and is required to detect differential radioresponses and align with specific proteomic alterations.

Identifying tumour-specific radiation-responsive proteins and thus also determining potential targets will be critical for developing targeted therapies that enhance radiation-induced death, specifically in tumour cells.

Here, we have presented a proteomic analysis of matched prospective human PCa tissue in response to therapeutic radiation. We observed that PCa tissue undergoes a detectible and conserved proteomic response to RT – supporting our initial hypothesis. This contributed to the increased expression of several known radiation-responsive pathways; including wound healing, immune activation and extracellular matrix remodelling. Determining if subtle variations in the dynamics and expression of these proteins and pathways predict for cancer recurrence following radiation will be the subject of further investigation. Pertinently, our study has established that proteomic analyses using fixed PCa tissue faithfully reflect those observed for fresh tissue, presenting an opportunity to confidently screen a large number of patients at a relatively low cost. Gathering a detailed understanding of the spectrum of proteomic responses to radiation, and assessing how these might be useful in targeted therapeutic approaches, is designed to increase curative success from frontline radiation treatments.

References

1.Blanchard, P., A. Briganti, and A. Bossi, *Re: Christopher J.D. Wallis, Refik Saskin, Richard Choo, et al. Surgery Versus Radiotherapy for Clinically-localized Prostate*

Cancer: A Systematic Review and Meta-analysis. Eur Urol 2016;70:21-30. Eur Urol, 2016. **70**(1): p. e15-6.
2.Chang, L., et al., *Emerging roles of radioresistance in prostate cancer metastasis and radiation therapy.* Cancer Metastasis Rev, 2014. **33**(2-3): p. 469-96.
3.Azimzadeh, O. and S. Tapio, *Proteomics approaches to investigate cancer radiotherapy outcome: slow train coming.* Translational Cancer Research, 2017.
4.Escher, C., et al., *Using iRT, a normalized retention time for more targeted measurement of peptides.* Proteomics, 2012. **12**(8): p. 1111-21.
5.Tyanova, S., et al., *The Perseus computational platform for comprehensive analysis of (prote)omics data.* Nat Methods, 2016. **13**(9): p. 731-40.
6.Kanehisa, M., et al., *KEGG: new perspectives on genomes, pathways, diseases and drugs.* Nucleic Acids Res, 2017. **45**(D1): p. D353-D361.
7.Kanehisa, M. and S. Goto, *KEGG: kyoto encyclopedia of genes and genomes.* Nucleic Acids Res, 2000. **28**(1): p. 27-30.
8.Kanehisa, M., et al., *KEGG as a reference resource for gene and protein annotation.* Nucleic Acids Res, 2016. **44**(D1): p. D457-62.
9.Chen, E.Y., et al., *Enrichr: interactive and collaborative HTML5 gene list enrichment analysis tool.* BMC Bioinformatics, 2013. **14**: p. 128.
10.Kuleshov, M.V., et al., *Enrichr: a comprehensive gene set enrichment analysis web server 2016 update.* Nucleic Acids Res, 2016. **44**(W1): p. W90-7.
11.Ashburner, M., et al., *Gene ontology: tool for the unification of biology. The Gene Ontology Consortium.* Nat Genet, 2000. **25**(1): p. 25-9.
12.Gene Ontology, C., *Gene Ontology Consortium: going forward.* Nucleic Acids Res, 2015. **43**(Database issue): p. D1049-56.
13.Mi, H., et al., *PANTHER version 11: expanded annotation data from Gene Ontology and Reactome pathways, and data analysis tool enhancements.* Nucleic Acids Res, 2017. **45**(D1): p. D183-D189.
14.Shannon, P., et al., *Cytoscape: a software environment for integrated models of biomolecular interaction networks.* Genome Res, 2003. **13**(11): p. 2498-504.
15.Bindea, G., et al., *ClueGO: a Cytoscape plug-in to decipher functionally grouped gene ontology and pathway annotation networks.* Bioinformatics, 2009. **25**(8): p. 1091-3.
16.Paul, P.J., et al., *Restoration of tumor suppression in prostate cancer by targeting the E3 ligase E6AP.* Oncogene, 2016. **35**(48): p. 6235-6245.
17.Dunne, J.C., et al., *Proteins from formalin-fixed paraffin-embedded prostate cancer sections that predict the risk of metastatic disease.* Clin Proteomics, 2015. **12**(1): p. 24.
18.Spenle, C., et al., *Tenascin-C: Exploitation and collateral damage in cancer management.* Cell Adh Migr, 2015. **9**(1-2): p. 141-53.
19.Zuliani-Alvarez, L. and K.S. Midwood, *Fibrinogen-Related Proteins in Tissue Repair: How a Unique Domain with a Common Structure Controls Diverse Aspects of Wound Healing.* Adv Wound Care (New Rochelle), 2015. **4**(5): p. 273-285.
20.Rosenkrans, W.A., Jr. and D.P. Penney, *Cell-cell matrix interactions in induced lung injury. IV. Quantitative alterations in pulmonary fibronectin and laminin following X irradiation.* Radiat Res, 1987. **109**(1): p. 127-42.
21.Lee, K.F., et al., *Gene expression profiling of biological pathway alterations by radiation exposure.* Biomed Res Int, 2014. **2014**: p. 834087.
22.Deloch, L., et al., *Modern Radiotherapy Concepts and the Impact of Radiation on Immune Activation.* Front Oncol, 2016. **6**: p. 141.
23.Surace, L., et al., *Complement is a central mediator of radiotherapy-induced tumor-specific immunity and clinical response.* Immunity, 2015. **42**(4): p. 767-77.

24.Widlak, P., et al., *Serum Proteome Signature of Radiation Response: Upregulation of Inflammation-Related Factors and Downregulation of Apolipoproteins and Coagulation Factors in Cancer Patients Treated With Radiation Therapy--A Pilot Study.* Int J Radiat Oncol Biol Phys, 2015. **92**(5): p. 1108-15.
25.Lukkahatai, N., et al., *Proteomic serum profile of fatigued men receiving localized external beam radiation therapy for non-metastatic prostate cancer.* J Pain Symptom Manage, 2014. **47**(4): p. 748-756 e4.
26.Loesch, K., et al., *Functional genomics screening utilizing mutant mouse embryonic stem cells identifies novel radiation-response genes.* PLoS One, 2015. **10**(4): p. e0120534.
27.Nishimura, Y., et al., *Radioprotection of mice by lactoferrin against irradiation with sublethal X-rays.* J Radiat Res, 2014. **55**(2): p. 277-82.
28.Shackley, D.C., et al., *Comparison of the cellular molecular stress responses after treatments used in bladder cancer.* BJU Int, 2002. **90**(9): p. 924-32.
29.Budworth, H., et al., *DNA repair and cell cycle biomarkers of radiation exposure and inflammation stress in human blood.* PLoS One, 2012. **7**(11): p. e48619.
30.Chang, L., et al., *Identification of protein biomarkers and signaling pathways associated with prostate cancer radioresistance using label-free LC-MS/MS proteomic approach.* Sci Rep, 2017. **7**: p. 41834.
31.Teresa Pinto, A., et al., *Ionizing radiation modulates human macrophages towards a pro-inflammatory phenotype preserving their pro-invasive and pro-angiogenic capacities.* Sci Rep, 2016. **6**: p. 18765.
32.Heutinck, K.M., et al., *Serine proteases of the human immune system in health and disease.* Mol Immunol, 2010. **47**(11-12): p. 1943-55.
33.Bok, R.A., et al., *Patterns of protease production during prostate cancer progression: proteomic evidence for cascades in a transgenic model.* Prostate Cancer Prostatic Dis, 2003. **6**(4): p. 272-80.
34.Mason, S.D. and J.A. Joyce, *Proteolytic networks in cancer.* Trends Cell Biol, 2011. **21**(4): p. 228-37.
35.Barker, H.E., et al., *The tumour microenvironment after radiotherapy: mechanisms of resistance and recurrence.* Nat Rev Cancer, 2015. **15**(7): p. 409-25.
36.Crockett, D.K., et al., *Identification of proteins from formalin-fixed paraffin-embedded cells by LC-MS/MS.* Lab Invest, 2005. **85**(11): p. 1405-15.

Figure legends

Figure 1: Proteomic analysis of pre- and radiation-treated human prostate tissue and sample cluster characteristics. (A) Study design outlining workflow for phase I (cluster analysis and candidate identification in three patients) and phase II (ontological analyses and candidate validation). Cluster analyses of individual Pre- and Post-radiation samples using (B) Hierarchical clustering analysis and (C) two-dimensional principal component analysis of normalised protein quantification levels. **P:** pre-treatment; **IR:** post-radiation.

Figure 2: Identification of conserved proteomic changes in response to radiation in fresh human prostate cancer tissue. Venn analysis of all significant candidate proteins in each patient with (A) exclusion and (B) inclusion of shared directionality criteria. (C) Stacked $\log_2$

fold changes for all 49 candidates in each patient. Increased: ≥1.5-fold; decreased: ≤ 1.5-fold. Black dots indicate 27 high confidence proteins with uniform directional changes.

Figure 3: Ontological analyses of proteins exhibiting differential abundance following HDRBT. Ontological classes from gene ontology consortium database include: (A) biological processes, (B) molecular functions and (C) cell compartment. (D) ClueGO / Cytoscape analysis of protein candidates with clustering on the basis of shared ontology groups.

Figure 4: Validation of 49 high-confidence radioresponsive proteins in extended cohort of formalin-fixed paraffin-embedded samples. (A) Mass spectrometric analysis of protein extracted from FFPE biopsies from seven additional patients and illustration of shared abundance changes. Dotted line indicates combined FFPE analysis of six patients. (B) Number of total protein identifications in each patient pair and proportional number of candidates identified and percentage validation of 49 protein candidate list. S.V statistically verified, n.s; not significant

Table 1: Serum PSA, Gleason, T-stage and age characteristics of cohort

Patient ID	Sample type(s)	Serum PSA (ng/ml)	Gleason Grade	T-stage	Age	Adjuvant therapy
RB031	Fresh and FFPE	9.3	3	1c	68	-
RB038	Fresh and FFPE	11.3	3	2c	70	ADT
RB045	Fresh	5.3	2	1c	49	-
RB006	FFPE	11.2	3	3a	67	-
RB008	FFPE	4.4	2	2a	73	-
RB016	FFPE	7.5	2	1c	57	-
RB019	FFPE	80	3	1c	60	ADT
RB020	FFPE	7.4	2	2b	71	-

FFPE: formalin-fixed paraffin-embedded, PSA: prostate-specific antigen, ADT: androgen-deprivation therapy

Table 2 Observed fold changes of 27 conserved proteomic changes in response to radiation

Gene	Protein Product	Function/Class	Fold-change			
			031	038	045	Average
FTL	Ferritin Light Chain	Iron storage macromolecule	4.63	6.15	27.90	12.89
TNC	Tenascin C	Secreted glycoprotein	5.07	18.41	3.29	8.92
KRT15	Keratin 15	Type I cytokeratin	20.86	3.34	1.81	8.67
FGB	Fibrinogen Beta Chain	Secreted glycoprotein	3.59	13.96	3.72	7.09
FGG	Fibrinogen Gamma Chain	Secreted glycoprotein	3.60	10.61	2.82	5.68
FN1	Fibronectin 1	Secreted glycoprotein	2.80	9.36	1.71	4.62
FGA	Fibrinogen Alpha Chain	Secreted glycoprotein	2.77	8.96	1.96	4.56
CD163	CD163 Molecule	Receptor	3.11	3.92	4.83	3.95
PLD3	Phospholipase D Family Member 3	Enzyme	2.23	1.88	5.60	3.24
FTH1	Ferritin Heavy Chain 1	Iron storage macromolecule	2.23	1.52	5.25	3.00
FDXR	Ferredoxin Reductase	Enzyme	2.61	3.26	3.11	2.99
CFB	Complement Factor B	Complement protein	5.47	1.55	1.56	2.86
HLA-DRA	Major Histocompatibility Complex, Class II, DR Alpha	Receptor	3.62	1.66	2.17	2.48
TYMP	Thymidine Phosphorylase	Enzyme	3.41	1.56	2.48	2.48
SFN	Stratifin	14-3-3 protein	1.73	2.96	2.54	2.41
APOA4	Apolipoprotein A4	Glycoprotein precursor	3.46	1.58	2.14	2.40
CTSB	Cathepsin B	Lysosomal cysteine protease	2.00	2.20	2.97	2.39
COL7A1	Collagen Type VII Alpha 1 Chain	Structural protein	2.81	1.81	2.20	2.28
MVP	Major Vault Protein	Vault complex	2.83	2.32	1.52	2.22
FERMT3	Fermitin Family Member 3	Kindlin family protein	2.32	2.12	2.09	2.18
CTSD	Cathepsin D	Lysosomal aspartyl protease	1.53	2.58	2.41	2.17
SERPINH1	Serpin Family H Member 1	Serine protease inhibitor	1.77	2.93	1.73	2.14
G6PD	Glucose-6-Phosphate Dehydrogenase	Enzyme	1.88	1.60	1.62	1.70
GPX1	Glutathione Peroxidase 1	Enzyme	1.60	1.53	1.65	1.59
ACLY	ATP Citrate Lyase	Enzyme	-1.83	-1.56	-1.53	-1.64
ACAT1	Acetyl-CoA Acetyltransferase 1	Enzyme	-2.69	-2.15	-1.90	-2.25
IQGAP2	IQ Motif Containing GTPase Activating Protein 2	Enzyme	-1.89	-2.83	-2.07	-2.26

Table 3: Protein coverage in biopsy pairs and candidate validation using fixed PCa tissue

	Candidates			Validation	
Patient	**Total number of proteins quantified**	**Number of candidates**	**%**	**Number validated**	**%**
Fresh tissue					
RB031	6239	1086	17.4	-	-
RB038	5109	376	7.4	-	-
RB045	5630	182	3.2	-	-
Shared	**4665**	-	-	-	
FFPE tissue					
RB031	4924	693	14.1	30	61.2
RB038	5087	262	5.2	27	55.1
RB06	5215	360	6.9	20	40.8
RB08	5004	101	2.0	13	26.5
RB016	5402	366	6.8	32	65.3
RB019	5353	325	6.1	30	61.2
RB020	5077	63	1.2	10	20.4
Shared	**3974**	-	-	-	-
Fresh/FFPE Overlap	**3706**	-	-	-	-

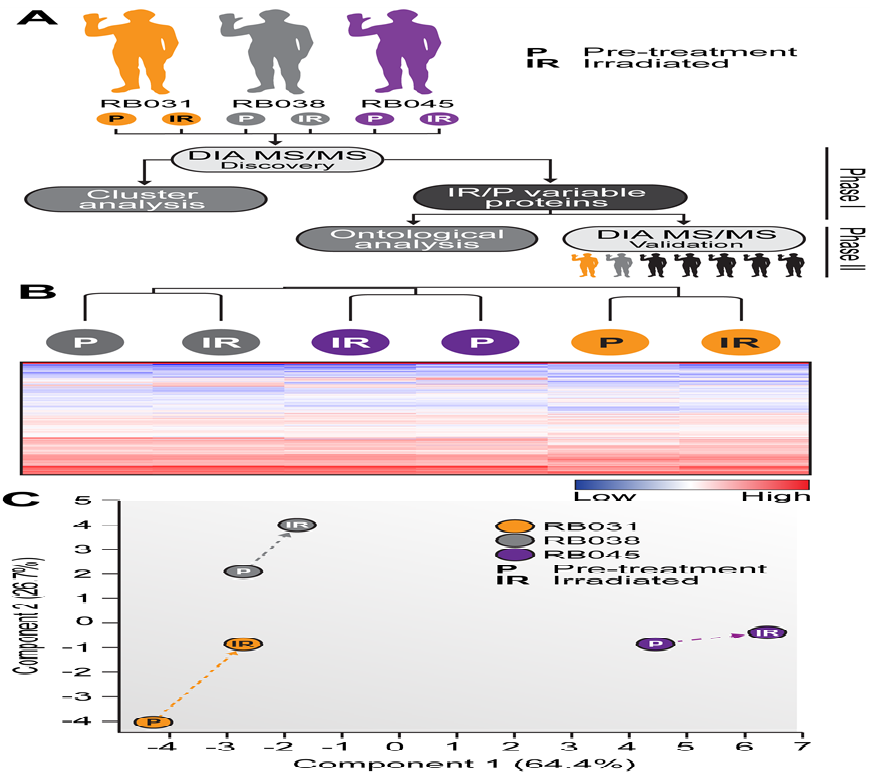

Figure1 .

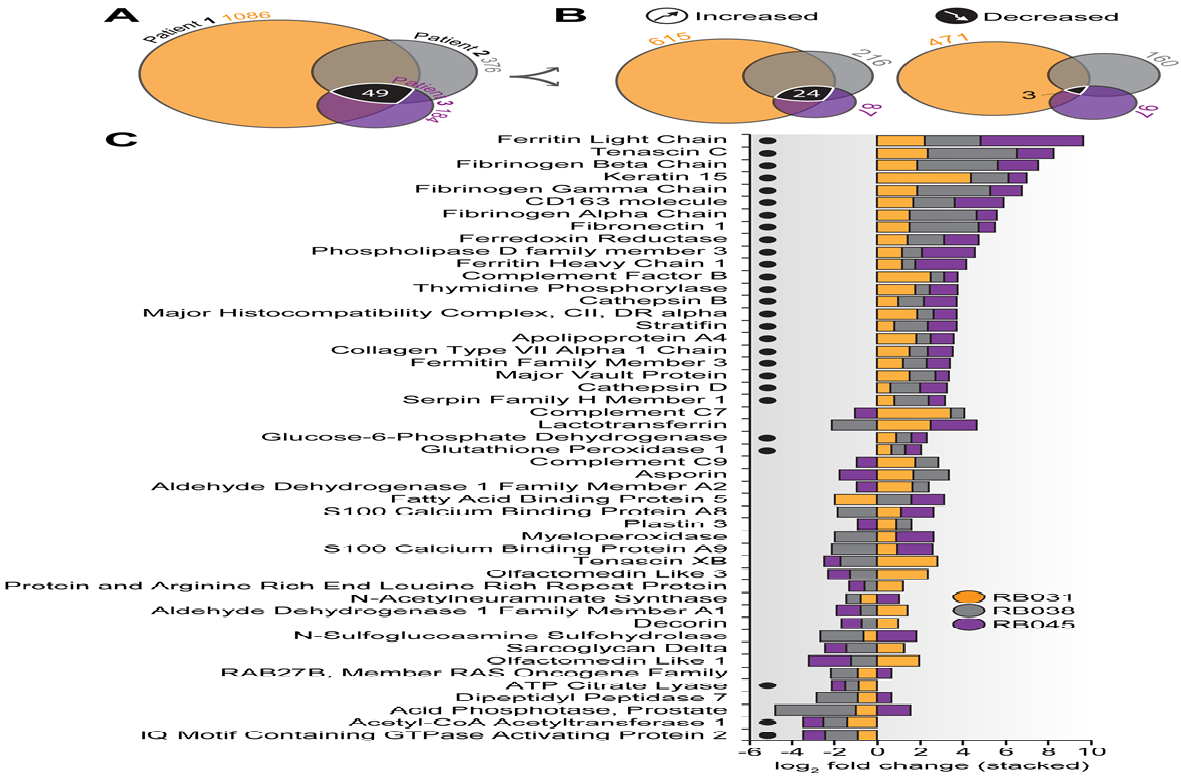

Figure2 .

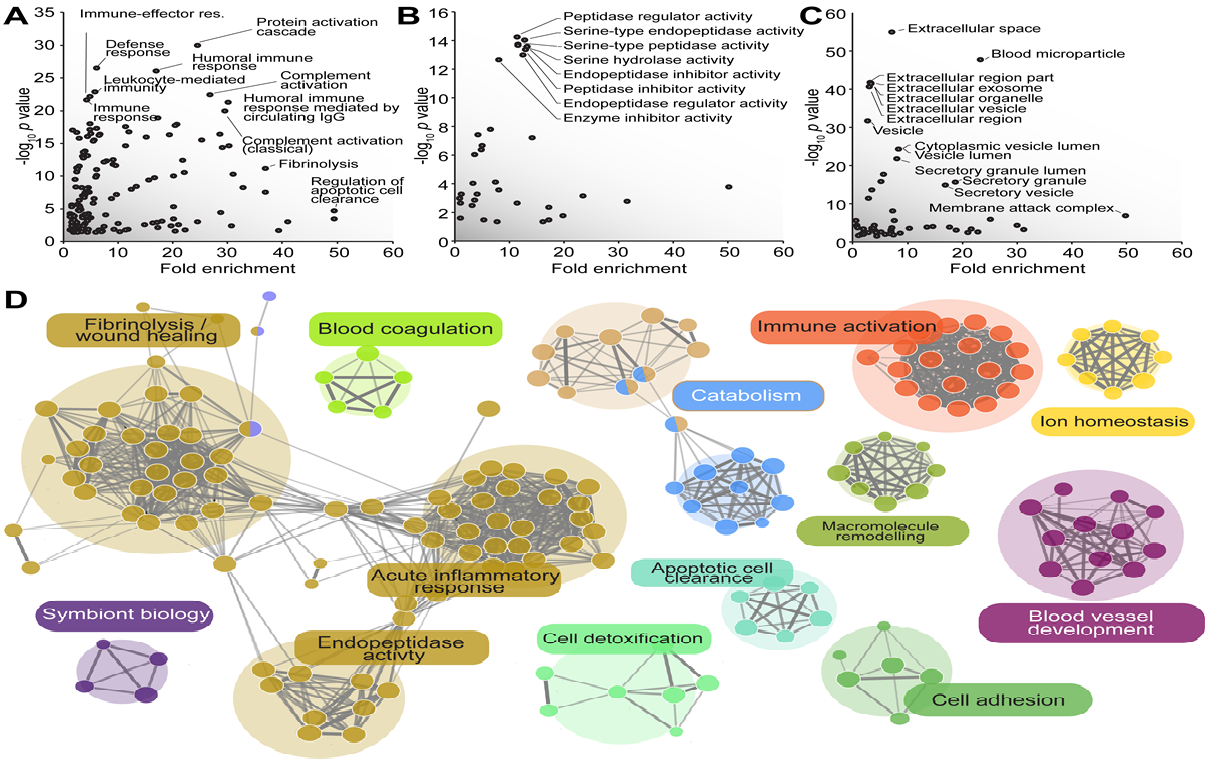

Figure3 .

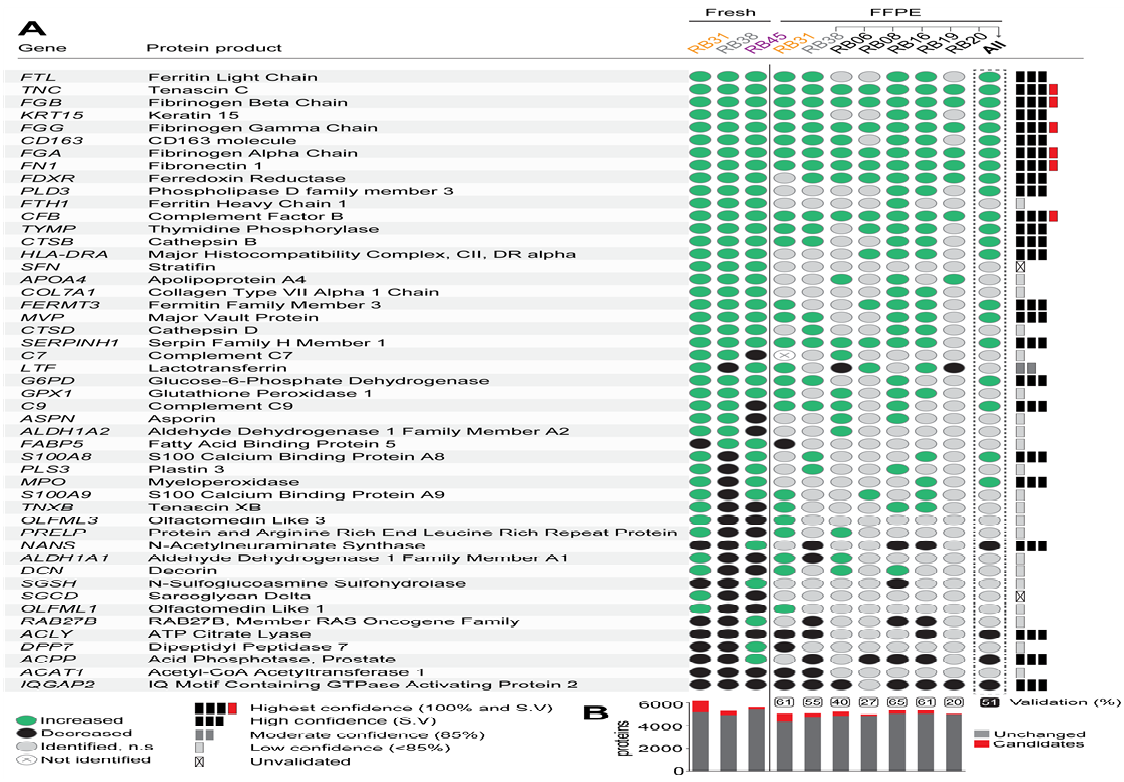

Figure4 .